Oncology Research, Vol. 27, pp. 911–921
Printed in the USA.

0965-0407/19 $90.00 + .00
DOI: https://doi.org/10.3727/096504019X15516966905337
E-ISSN 1555-3906
www.cognizantcommunication.com

miR-148-3p Inhibits Growth of Glioblastoma Targeting DNA Methyltransferase-1 (DNMT1)

Yongtao Li,* Fanyu Chen,* Jiancheng Chu,* Chao Wu,* Yuan Li,† Heng Li,† and Hongxin Ma*

*Department of Neurosurgery, Tengzhou Central People's Hospital, Tengzhou, Shandong, P.R. China
†School of Medicine, Shandong University, Jinan, Shandong, P.R. China

To date, miR-148-3p and DNMT1–recombinant human runt-related transcription factor 3 (RUNX3) axis have been linked to cell proliferation, migration, and invasion; however, their roles and relationships in human glioblastoma multiforme (GBM) are still not clear. Here we found that the expression of miR-148-3p in glioma tissues was decreased compared with adjacent nontumor tissues and correlated with WHO grade, tumor size, and prognosis as well as DNMT1 and RUNX3 expressions. Compared with NHA cells, the expression of miR-148-3p in U87 and U251 cells was also downregulated and accompanied with upregulation of DNMT1 and hypermethylation level of RUNX3 promoter region. miR-148-3p overexpression induced apoptosis and cell cycle arrest of U87 and U251 cells, and affected cell migration and invasion. miR-148-3p mimics effectively suppressed the expression of DNMT1 and methylation of RUNX3 promoter, finally upregulating RUNX3 expression. Mechanistically, the 3 -untranslated region (3 -UTR) of DNMT1 was a direct target of miR-148-3p. Overexpression of miR-148-3p or inhibition of DNMT1 induced the expression of E-cadherin and reduced the expressions of N-cadherin, vimentin, MMP-2, and MMP-9. In conclusion, miR-148-3p directly repressed the expression of DNMT1 and inhibited proliferation, migration, and invasion by regulating DNMT1–RUNX3 axis and the epithelial–mesenchymal transition in GBM. Our findings provide a new foundation for treatment of patients with GBM.

Key words: miR-148-3p; DNMT; RUNX3; Glioblastoma multiforme (GBM)

INTRODUCTION

Gliomas are the most frequent primary brain tumors in adults[1,2]. Malignant gliomas, especially glioblastomas, are aggressive and lethal neoplasms characterized by rapid growth and persistent infiltration, which means that a radical resection is almost impossible[3,4]. A majority of patients are often diagnosed at an advanced or metastatic stage, which makes this disease difficult to cure. Although unlimited proliferation and inhibition of tumor cell apoptosis have been recognized as the key reasons for the malignant growth of gliomas, the underlying epigenetic and genetic changes are still poorly understood[5,6]. To date, prognostic biomarkers and therapeutic targets for gliomas have not been fully characterized.

miRNAs are a family of small noncoding RNAs, which regulate the expression of various oncogenes or tumor suppressor genes via complementarily binding to regulatory regions of target genes[7]. The expression profiling of miRNAs has already been suggested as diagnostic and prognostic biomarkers to assess tumor initiation, progression, and response to treatment in cancer patients[8]. A previous study showed that miR-148a suppresses human renal cell carcinoma malignancy by targeting AKT2[9]. Luo et al. also suggested that miR-148a acts as a tumor suppressor of cutaneous squamous cell carcinoma via inhibiting MAPK pathway[10]. However, the role of miR-148-3p in GBM is still unclear. DNA methylation is established by DNA methyltransferases, of which DNMT1 maintains methylation patterns, and can be downregulated posttranscriptionally by the miR-148 family[11]. To date, DNMT1 has been suggested to play a role in the pathogenesis of GBM[12,13]. However, it is not clear whether miR-148-3p can mediate the progression of GBM via regulating DNMT1 expression.

In this study, we investigated the molecular mechanisms underlying miR-148-3p-mediated recombinant human runt-related transcription factor 3 (RUNX3) methylation in GBM cell lines. We identified that miR-148-3p suppressed

Address correspondence to Hongxin Ma, Department of Neurosurgery, Tengzhou Central People's Hospital, No.181 Xingtan Road, Tengzhou, 277500 Shandong, P.R. China. E-mail: mahongxintengzhou@163.com

DNMT1 expression to upregulate the expression of RUNX3, which further inhibited migration or invasion, and induced apoptosis of GBM cells.

MATERIALS AND METHODS

Tissue Specimens

Forty cases of gliomas tissues (21 males and 19 females; age range, 31–68 years old; median age, 50 years old) were obtained from Tengzhou Central People's Hospital (Tengzhou, Shandong, P.R. China). Patients who underwent chemotherapy and radiotherapy were excluded. To analyze overall survival, these samples were divided into two groups (low group and high group) according to the median value. All of the samples and clinical data were obtained with the written informed consent from patients or their guardians. This study was approved by the ethics committees of Tengzhou Central People's Hospital and conducted according to the principles of Helsinki Declaration. All collected tissue samples were rapidly snap frozen in liquid nitrogen and stored in liquid nitrogen at –80°C.

Cell Culture and Reagents

NHA, U87, U251, and human embryonic kidney 293T (HEK-293T) cell lines were purchased from the American Type Culture Collection (ATCC, Manassas, VA, USA), and cells were grown in Dulbecco's modified Eagle's medium (DMEM) or L15 medium (Gibco Laboratories, Grand Island, NY, USA). All cells were cultured at 37°C in a humidified incubator containing 5% CO_2, supplemented with 10% fetal bovine serum (Gibco, Carlsbad, CA, USA). 5-Azacytidine (5-Aza), a methyltransferase inhibitor (Sigma-Aldrich, St. Louis, MO, USA), was also used for treating cells as the positive control.

Cell Transfection

For cell transfection, miR-148-3p mimics were purchased from Guangzhou RuiBo Biological Company (Guangzhou, P.R. China). Cells were transfected with miR-148-3p mimics (30 nmol/L) or miR-148-3p negative controlled (miR-NC) sequences (30 nmol/L) using Lipofectamine 2000 kit (Invitrogen, Carlsbad, CA, USA) following the manual instructions. NC (scramble) sequences were used as the control. Transfections were carried out using Lipofectamine 2000 reagent (Invitrogen) according to the manufacturer's instructions.

Quantitative RT-PCR Analysis

Total RNA was extracted from fresh tissues and cells using TRIzol reagent (Thermo Fisher Scientific, Rockford, IL, USA). Reverse transcription was performed using an RNA PCR Kit (AMV; TaKaRa, Otsu, Japan). Quantitation of miRNAs and mRNA was carried out by qRT-PCR using SYBR Premix Ex Taq™ (TaKaRa) according to the manufacturer's instructions. U6 was used as the internal control for miR-148-3p expression levels. GAPDH was used as an internal control for other genes' mRNA expression. The primers for qRT-PCR detection of genes were synthesized by TaKaRa. The fold changes in expression were calculated using the $2^{-\ Ct}$ method.

Flow Cytometry

Apoptosis was examined by flow cytometric analysis. An Annexin V–FITC/PI double stain assay (BD Biosciences, San Jose, CA, USA) was performed following the manufacturer's protocol. The analysis was performed with FlowJo software (Treestar, Inc., San Carlos, CA, USA). All the assays were performed in triplicate.

Cell Cycle Analysis

To analyze the effect of miR-148-3p on cell cycle, the transfected cells were detached and fixed in 1 ml of cold 70% ethanol in PBS for 24 h. The cells were washed once with 3 ml of PBS. Fixed cells were resuspended in 1 mg/ml of propidium iodide (BD Biosciences) and 0.5 mg/ml of RNaseA (Keygen Biotech, Nanjing, P.R. China) in PBS for 30 min at 37°C. Approximately 1.5×10^5 cells were analyzed by a CyFlow® flow cytometer (BD Biosciences).

Transwell Assay

To analyze the effect of miR-148-3p on cell invasion, the transfected cells were detected by the assays of invasion. The top of the Transwell chambers was covered with 0.5 mg/ml of Matrigel (BD Biosciences). The cell lines were transferred to the top of the Transwell chambers in serum-free DMEM medium (1×105 cells/pore). DMEM containing 5% FBS was added to the lower chambers as a cell-inducible factor. In the cultured system, cells were cultured after 48 h, and unpenetrated cells were removed from the top wells using a cotton ball. Cells on the lower membrane surface of the Transwell chambers were fixed in 4% formaldehyde and stained with 0.2% crystal violet (Biosun Biotech, Shanghai, P.R. China). Invading cells were manually counted in eight randomly chosen fields under a microscope, and photographs were taken.

Dual-Luciferase Reporter Assay

Cells were seeded in 96-well plates (5×10^3 cells/well) and incubated at 37°C for 48 h. miR-148-3p mimics and miR-NC were cotransfected with the reporter vector DNMT1 wild-type (3 -UTR-WT) or DNMT1 mutated-type (3 -UTR-MUT) into the HEK-293T cells. Luciferase activity was measured using the Dual-Luciferase® Reporter Assay System Protocol (Promega Corporation, Fitchburg, WI, USA).

Western Blot Analysis

Treated cells were lysed with radioimmunoprecipitation assay buffer (Beyotime Institute of Biotech,

Shanghai, P.R. China), containing proteinase inhibitors. After centrifugation at 12,000 rpm for 15 min at 4°C, the supernatant was collected, and the protein concentrations were determined by a BCA kit (Beyotime Institute of Biotech). Total protein was separated by 10% SDS-PAGE and then transferred to PVDF membranes (Sigma-Aldrich). After blocking with 5% low-fat dried milk for 2 h at room temperature, membranes were incubated overnight with the appropriate primary antibodies (1:1,000; Santa Cruz Biotechnology, Santa Cruz, CA, USA). The membranes were then washed in PBS three times and incubated with the corresponding horseradish peroxidase-conjugated secondary antibodies (Santa Cruz Biotechnology) for 2 h at room temperature. GAPDH was used as an internal control, and signals were detected by enhanced chemiluminescent reagents.

Methylation-Specific PCR (MSP)

The RASSF1A methylation statuses of cells were determined by a methylation-specific PCR assay. Genomic DNA of tissues and cells was isolated by the Get pure DNA Kit (Dojindo Molecular Technologies, Kumamoto, Japan) by following the instruction of the manufacturer. Genomic DNA is treated with bisulfate. Bisulfate converts cytosine into a uracil base, but has no effect on methylated cytosine. We thus used the MSP assay to differentiate between methylated and nonmethylated DNA in a Hot-Star TaqE PCR machine (TaKaRa).

Statistical Analysis

The results were reported as the mean ± standard deviation (SD). Statistical analyses were performed using the GraphPad Prism 6.0 statistical software (GraphPad Software, Inc., San Diego, CA, USA). The p values were calculated using the Student's t-test or one-way analysis of variance (ANOVA). Significance was defined as a value of $p < 0.05$.

RESULTS

Expression Status of miR-148-3p–DNMT1–RUNX3 Axis in Glioma Tissues

To determine the expression of miR-148-3p in glioma tissues, qRT-PCR was performed. The results validated that miR-148-3p expression in glioma tissues obviously decreased compared with adjacent nontumor tissues ($p < 0.001$) (Fig. 1A). Then we performed Western blot to analyze the expressions of DNMT1 and RUNX3 proteins in the resected cancer tissues and adjacent nontumor tissues. Western blot analysis revealed higher expression level of DNMT1 protein in glioma tissues compared with adjacent nontumor tissues ($p < 0.001$) (Fig. 1B). Inversely, the expression level of RUNX3 protein was downregulated in glioma tissues than that in adjacent nontumor tissues ($p < 0.001$) (Fig. 1B).

miR-148-3p Correlates With DNMT1–RUNX3 Axis in Glioma Tissues

To further investigate the relationship among miR-148-3p, DNMT1, and RUNX3 in glioma tissues, Spearman's correlation analysis was carried out, which further demonstrated that miR-148-3p expression level was negatively correlated with DNMT1 expression levels in glioma tissues ($R^2 = 0.708$, $p < 0.001$) (Fig. 1C). On the contrary, miR-148-3p expression level positively correlated with RUNX3 protein expression level in glioma tissues ($R^2 = 0.616$, $p < 0.001$) (Fig. 1D). These results suggested that downregulation of miR-148-3p may be associated with upregulation of DNMT1 in GBM.

Associations of miR-148-3p–DNMT1–RUNX3 Axis With Clinicopathological Features and Prognosis of Patients With Gliomas

We analyzed the relationship between miR-148-3p–DNMT1–RUNX3 axis and the clinicopathological characteristics of patients with gliomas. We found that miR-148-3p–DNMT1–RUNX3 axis significantly correlated with WHO grade (all $p < 0.05$) and tumor size (all $p < 0.05$) in patients with gliomas (Table 1). No significant correlations were observed between miR-148-3p–DNMT1–RUNX3 axis and other clinicopathologic variables, such as age, gender, necrosis, tumor size, and cystic change ($p > 0.05$) (Table 1). Kaplan–Meier survival model showed that the overall survival duration of patients with gliomas in the high miR-148-3p or RUNX3 expression group was longer than that in the low expression group ($p = 0.007$, 0.049, respectively) (Fig. 1E). Inversely, the overall survival duration of patients with gliomas in the low DNMT1 expression group was longer than that in the high expression group ($p = 0.046$) (Fig. 1E). Using a Cox proportional hazard model, we analyzed each variable with overall survival of patients with gliomas. Finally, univariate and multivariate analysis validated that miR-148-3p–DNMT1–RUNX3 axis was the independent predictors of prognosis in patients with gliomas (Table 2).

Expression Status of miR-148-3p–DNMT1–RUNX3 Axis in GBM Cells

To determine the potential miR-148-3p–DNMT1–RUNX3 axis in GBM cell lines, we first investigated the expressions of miR-148-3p and DNMT1 using NHA, U87, and U251 cell lines. We found that the expression of miR-148-3p was markedly decreased in U87 and U251 cell lines ($p < 0.001$) (Fig. 2A).

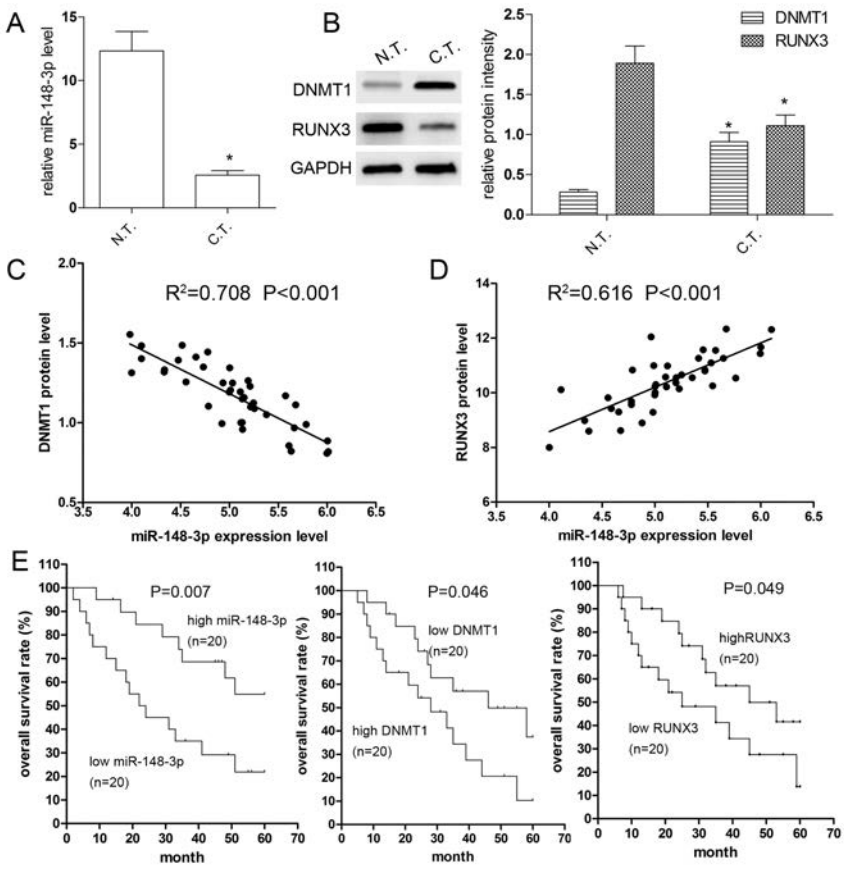

Figure 1. Expression and association of miR-148-3p, DNMT1, and recombinant human runt-related transcription factor 3 (RUNX3) in gliomas tissues. (A) qRT-PCR was performed to detect the expressions of miR-148-3p in 40 cases of gliomas tissues. (B) Western blotting was used to detect DNMT1 and RUNX3 protein level in gliomas tissues. Relative grayscale values of Western blotting were calculated to analyze the protein levels. U6 and GAPDH were used as internal controls, respectively. (C, D) Spearman's correlation analysis was carried out to investigate the relationship among miR-148-3p, DNMT1, and RUNX3 in 40 cases of gliomas tissues. (E) Survival analysis was conducted by Kaplan–Meier survival analysis. Asterisks indicated statistically significant differences. Data were represented as means ± SD. N.T., normal tissues; C.T., cancer tissues. *$p < 0.001$, versus control.

In addition, as shown in Figure 2B, DNMT1 mRNA expression was significantly increased in U87 and U251 cell lines compared with that in NHA cells. To further validate the methylation status of RUNX3 gene promoter and regulation of RUNX3 in human GBM, RUNX3 expression was further detected by qRT-PCR. The expression level of RUNX3 mRNA was significantly lower in U87 and U251 cells compared with that in NHA cells ($p < 0.001$) (Fig. 2C). In addition, methylation of RUNX3 was analyzed by MSP. Results showed that methylation levels of RUNX3 were increased in U87 and U251 cells compared with that in NHA cells ($p < 0.001$) (Fig. 2D). Western blot further validated the expressions of DNMT1 and RUNX3 proteins ($p < 0.001$) (Fig. 2E and F). Functionally, U87 and U251 cells exhibited a better migration and invasion capacity than NHA cells ($p < 0.001$) (Fig. 2G and H). Thus, U87 and U251 cells were chosen for the subsequent studies.

miR-148-3p or 5-Aza Downregulates DNMT1 and Upregulates RUNX3 Expression

First, to identify the DNMT1–RUNX3 axis in U87 and U251 cells, we treated cells with 10-μM 5-Aza. 5-Aza is a deoxycytidine analog that is typically used to activate methylated and silenced genes by promoter demethylation[14]. Here we used it as a positive control. We found that administration of cells with 5-Aza significantly decreased DNMT1 expression and elevated RUNX3 expression ($p < 0.001$) (Fig. 3A and B). To clarify the mechanism by which miR-148-3p played a tumor-suppressive role in migration and invasion of U87 and U251 cells, we transfected miR-148-3p mimics into U87 and U251 cells to overexpress miR-148-3p

Table 1. Correlation Among miR-148-3p, DNMT1, and RUNX3 Expression and Clinicopathological Factors of Patients With Gliomas

Indicators	Case	miR-148-3p	*p*	DNMT1 Protein	*p*	RUNX3 Protein	*p*
Age (years)			0.390		0.205		0.117
<50	20	10.09 ± 1.56		0.88 ± 0.28		1.15 ± 0.11	
50	20	9.82 ± 0.99		0.93 ± 0.29		1.02 ± 0.12	
Gender			0.439		0.134		0.098
Male	21	9.98 ± 0.93		0.92 ± 0.13		1.09 ± 0.13	
Female	19	10.21 ± 1.35		0.86 ± 0.17		1.13 ± 0.12	
Necrosis			0.135		0.103		0.122
Absence	25	10.32 ± 1.67		0.63 ± 0.17		1.13 ± 0.13	
Presence	15	9.61 ± 1.58		0.91 ± 0.19		1.08 ± 0.11	
Cystic change			0.188		0.005		0.012
Absence	27	12.15 ± 1.22		0.79 ± 0.08		1.29 ± 0.13	
Presence	13	6.36 ± 0.99		1.13 ± 0.14		0.99 ± 0.09	
Tumor size (cm)			0.003		0.001		0.003
<5 cm	26	14.67 ± 1.33		0.75 ± 0.07		1.21 ± 0.13	
5 cm	14	7.86 ± 0.68		1.06 ± 0.12		0.86 ± 0.09	
WHO grade			< 0.001		<0.001		< 0.001
I–II	28	12.39 ± 1.24	< 0.001	0.79 ± 0.21	<0.001	1.33 ± 1.17	< 0.001
III–IV	12	6.45 ± 0.73		1.28 ± 0.17		0.95 ± 0.09	

(Fig. 3A and B). The qRT-PCR analysis revealed that miR-148-3p overexpression remarkably decreased the expression of DNMT1 mRNA compared with miR-NC ($p < 0.001$) (Fig. 3A and B). In addition, the expression level of RUNX3 mRNA was increased in miR-148-3p-overexpressed U87 and U251 cells compared with that of miR-NC ($p < 0.001$) (Fig. 3A and B). These findings indicated that miR-148-3p may have the same function as 5-Aza. Subsequently, miR-148-3p transfection or 5-Aza administration decreased the expression of DNMT1 protein and increased the expression of RUNX3 protein in U87 cells ($p < 0.001$) (Fig. 3C) or U251 cells ($p < 0.001$) (Fig. 3D). Notably, the treatment of miR-148-3p combined with 5-Aza further suppressed DNMT1 and enhanced RUNX3 expression ($p < 0.001$) (Fig. 3D).

miR-148-3p or 5-Aza Reduces Methylation Level of RUNX3

As DNMT1 has been known as a DNA methyltransferase, we hypothesized that miR-148-3p reduced DNMT1 levels, and in turn altered RUNX3 methylation level and increased RUNX3 expression. A further investigation on DNA methylation level of RUNX3 promoter showed that miR-148-3p or 5-Aza significantly suppressed DNA methylation ($p < 0.001$) (Fig. 4A and B). Subsequently, we carried out methylation-specific PCR to examine RUNX3 methylation level and observed that, in both U87 and

Table 2. Univariate and Multivariate Cox Regression Analysis of Overall Survival

	Univariate Analysis		Multivariate Analysis	
Variables	HR (95% CI)	*p*	HR (95% CI)	*p*
Age (years, 50 vs. <50)	1.402 (0.864–2.274)	0.171		
Gender (male vs. female)	1.122 (0.766–1.645)	0.553		
Tumor size (cm, >5 vs. 5 cm)	2.065 (1.187–3.593)	0.011*		
Cystic change (absence vs. presence)	0.885 (0.574–1.364)	0.579		
Necrosis (absence vs. presence)	1.863 (0.935–3.057)	0.234		
WHO grade (III + IV vs. I + II)	2.611 (1.725–3.952)	< 0.001*	2.118 (1.354–3.312)	0.002*
miR-148-3p	2.811 (1.672–4.725)	< 0.001*	2.796 (1.717–4.553)	0.001*
DNTM1	2.549 (1.555–4.178)	< 0.001*	2.710 (1.681–4.368)	<0.001*
RUNX3	2.612 (1.499–4.552)	< 0.001*	2.765 (1.491–4.416)	<0.001*

HR, hazard ratio; CI, confidence interval.
*Statistically significant result.

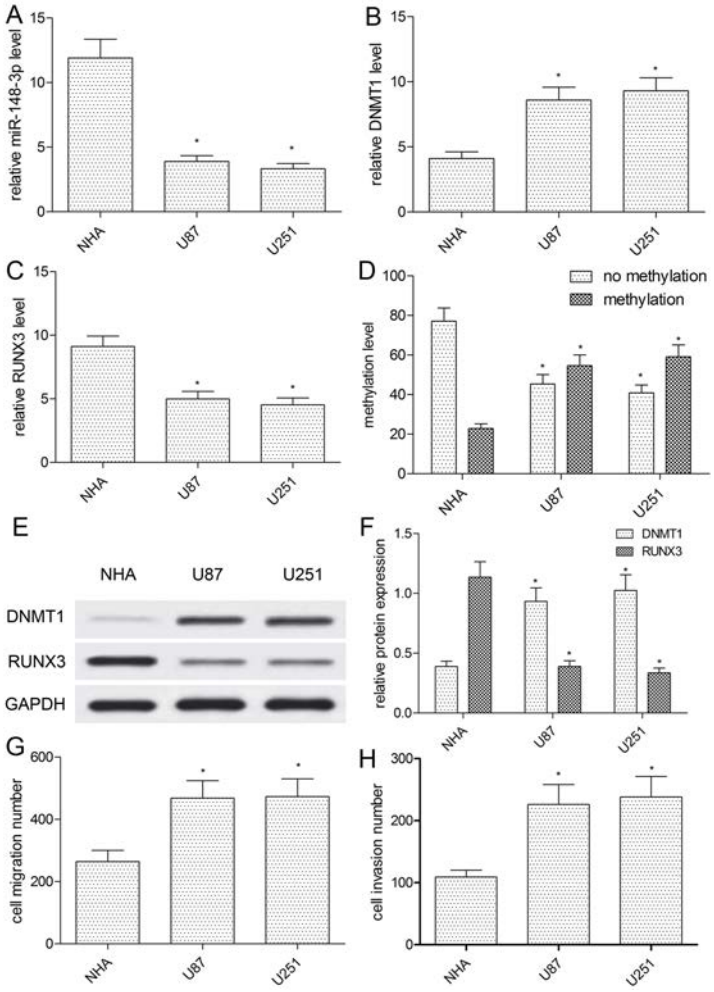

Figure 2. RUNX3 DNA methylation level, DNMT1, and miR-148-3p expression and migration potency in glioblastoma multiforme (GBM) cell lines. (A–C) Relative mRNA levels of miR-148-3p, DNMT1, and RUNX3 in three cell lines including NHA, U87, and U251 were measured by qRT-PCR. (D) DNA methylation level of RUNX3 gene promoter among NHA, U87, and U251 cells was detected by MSP. (E, F) Western blot bands of DNMT1 and RUNX3 proteins in NHA, U87, and U251 cells were analyzed semiquantitatively. (G) Transwell assay was used for cell migration of NHA, U87, and U251 cells. (H) Transwell assay was used for cell invasion of NHA, U87, and U251 cells. $*p < 0.01$ using one-way analysis of variances (ANOVA) followed by Tukey post hoc comparison.

U251 cells, miR-148-3p or 5-Aza substantially decreased the methylation level of RUNX3, whereas nonmethylated RUNX3 levels were increased in miR-148-3p-overexpressed or 5-Aza-treated cells ($p < 0.001$) (Fig. 4A and B). Notably, the treatment of miR-148-3p combined with 5-Aza effectively and largely decreased the methylation level of RUNX3 promoter ($p < 0.001$) (Fig. 4A and B). Taken together, miR-148-3p or 5-Aza could result in decreased expression of DNMT1, and then reduced methylation level of RUNX3, finally thereby increasing RUNX3 levels.

miR-148-3p Directly Targets 3 -UTR region of DNMT1

Since miRNAs regulate gene expression by targeting 3 -UTR region of mRNAs, we hypothesized that miR-148-3p was likely to bind 3 -UTR of DNMT1. The bioinformatic prediction revealed that miR-148-3p could target 3 -UTR of DNMT1 by complementary sequences (Fig. 4C). Dual-luciferase reporter assay showed that miR-148-3p only caused significant decrease (by ~50%) in wild-type 3 -UTR-fused luciferase reporter, not mutant 3 -UTR-fused luciferase reporter ($p > 0.05$) (Fig. 4D). These findings indicated that miR-148-3p may inhibit DNMT1 expression to suppress methylation of tumor suppressor gene RUNX3 promoter region, thus upregulating its gene expression.

miR-148-3p or 5-Aza Mediates Apoptosis and Cell Cycle

U87 and U251 cells were treated with miR-NC, miR-148-3p mimics, or 5-Aza. As expected, miR-148-3p mimics had a strong active effect on miR-148-3p mRNA

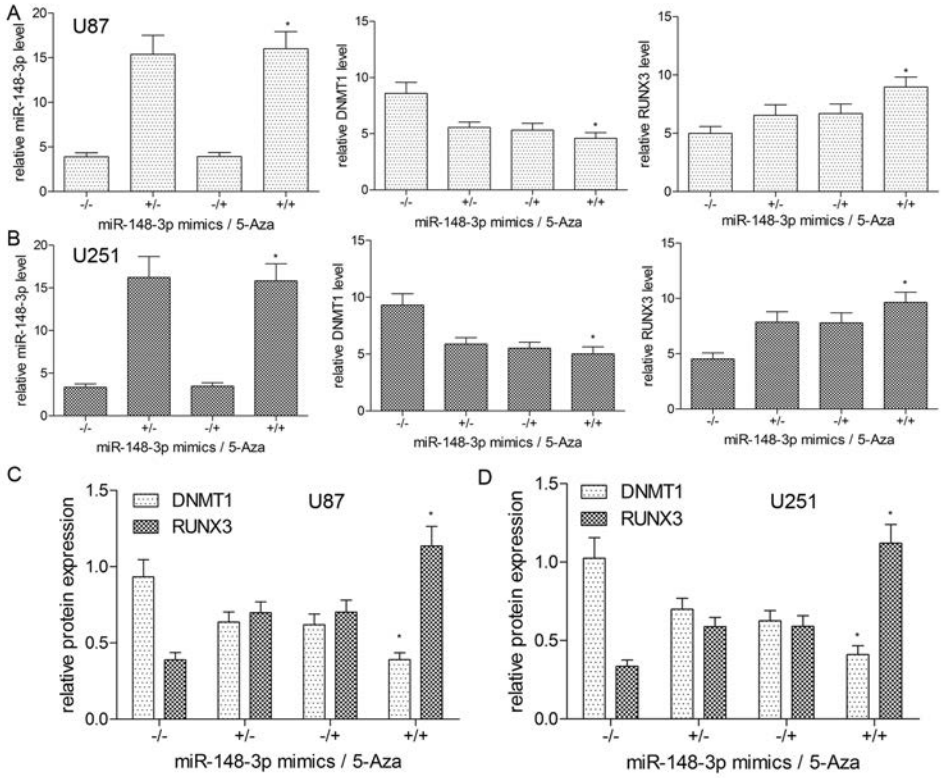

Figure 3. miR-148-3p mediates the mRNA and protein expressions of DNMT1 and RUNX3 in GBM cells. (A) qRT-PCR showed relative expression of miR-148-3p, DNMT1, and RUNX3 transcript in U87 cells after miR-148-3p mimics transfection and/or 5-Aza treatment. (B) qRT-PCR results in U251 cells. (C) Western blot bands for DNMT1 and RUNX3 proteins in U87 cells were analyzed semiquantitatively. (D) Western blot bands for DNMT1 and RUNX3 proteins in U251 cells were analyzed semiquantitatively. All data were presented as mean ± SD from three biological replicates. $*p < 0.01$ using one-way ANOVA followed by Tukey post hoc test.

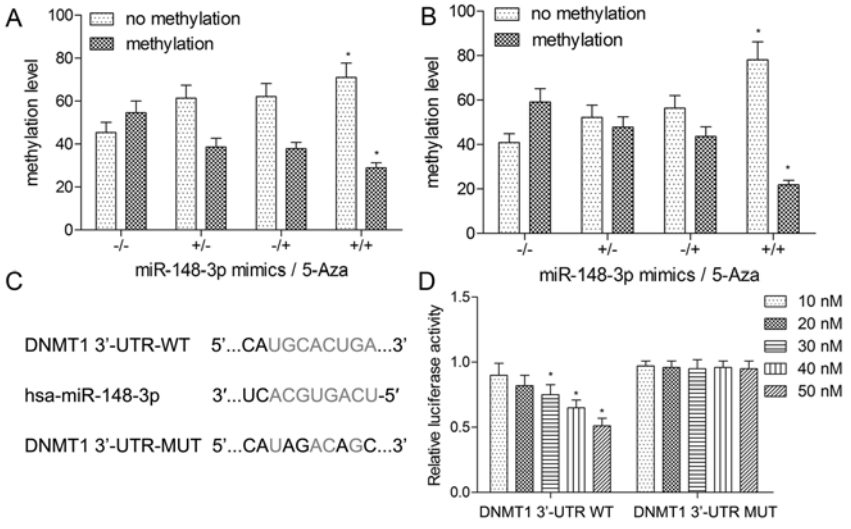

Figure 4. miR-148-3p mediates RUNX3 methylation and DNMT1 protein expression and targets 3 -untranslated region (3 -UTR) of DNMT1. (A) DNA methylation level after miR-148-3p mimics/5-Aza in U87 cell lines. (B) DNA methylation level after miR-148-3p mimics/5-Aza in U251 cell lines. (C) Sequence prediction between miR-148-3p and DNMT1 gene. (D) Relative luciferase activity in HEK-293T cells after cotransfection with miR-148-3p mimics and DNMT1 3 -UTR [wild type (WT) or mutated type (MUT)]. All data were presented as mean ± SD from three biological replicates. $*p < 0.01$ using one-way ANOVA followed by Tukey post hoc test.

expression. Then cell apoptosis was measured by flow cytometry using Annexin V–FITC and PI double staining. Flow cytometry analysis revealed that miR-148-3p or 5-Aza obviously influenced cell apoptosis compared with their respective miR-NC and control groups ($p < 0.01$) (Fig. 5A). Then we explored whether miR-148-3p was related to cell cycle progression in U87 and U251 cells, and flow cytometry was performed. The miR-148-3p-overexpressed or 5-Aza-treated cells displayed a dramatically higher number of cells in G_0/G_1 phase compared with their control cells ($p < 0.01$) (Fig. 5B and C), suggesting that miR-148-3p or 5-Aza regulates G_0/G_1 phase arrest.

miR-148-3p or 5-Aza Mediates Migration and Invasion

Transwell assay was then employed to gain an insight into the role of miR-148-3p or 5-Aza on the migration and invasion of U87 and U251 cells. As presented in Figure 5D and E, the number of migrated and invaded U87 cells was significantly reduced after transfection of miR-148-3p or/and 5-Aza administration ($p < 0.001$). In addition, overexpression of miR-148-3p or/and 5-Aza administration also significantly enhanced the migratory and invasive capacities of U251 cells ($p < 0.001$).

Effects of miR-148-3p or 5-Aza on the Epithelial–Mesenchymal Transition (EMT)-Related Proteins

To explore the role of miR-148-3p in EMT of GBM cells, the epithelial or mesenchymal markers in miR-148-3p-overexpressing U87 and U251 cells were measured by Western blot assay. As shown in Figure 6, a marked reduction in N-cadherin and vimentin expression was found in miR-148-3p-overexpressed or 5-Aza-administrated U87 and U251 cells compared with that of the control cells, whereas transfection of miR-148-3p or/and 5-Aza administration resulted in upregulation of epithelial marker, E-cadherin, compared with control ($p < 0.001$). Further invasion-associated markers were measured by Western blot analysis. The results revealed that transfection of miR-148-3p or/and 5-Aza administration decreased the level of MMP-2 and MMP-9 ($p < 0.001$) (Fig. 6A and B). These findings indicated that transfection of miR-148-3p or/and 5-Aza administration inhibits mesenchymal phenotypes of GBM cells, which indicates that miR-148-3p plays an essential role in the EMT process.

DISCUSSION

In recent years, miRNAs have been demonstrated to play a critical role in the progression of cancers by regulating the expressions of various oncogenes and tumor suppressors[15–19]. It has been reported that some miRNAs are involved in tumor invasion and metastasis[20], and the aberrant expressions of miRNAs are significantly related to the development and progression of GBM. Mechanistically, miRNAs interrupt cellular signaling pathways and inhibit the activity of tumor suppressor genes[21]. Notably, the expression of miR-148-3p has been found to be significantly downregulated in multiple

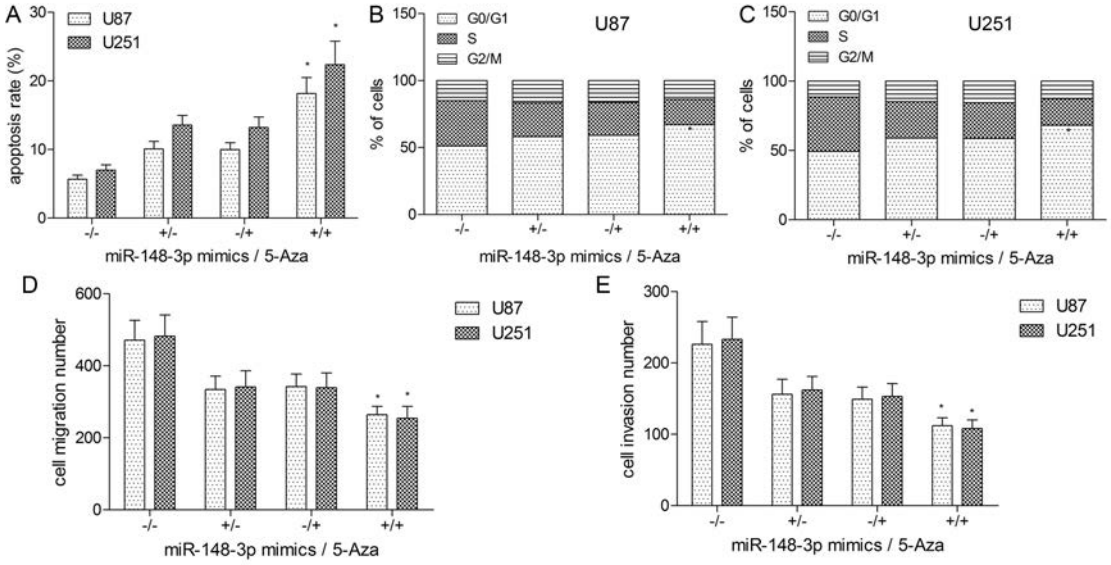

Figure 5. miR-148-3p mediated cell apoptosis, cell cycle arrest, migration, and invasion. (A) Flow cytometry analysis using annexin V/PI double-labeling approach to examine the apoptosis of U87 and U251 cells after miR-148-3p transfection and/or 5-Aza treatment. (B) Quantification of apoptotic rate by flow cytometry in U87 cells. (C) Quantification of apoptotic rate by flow cytometry in U251 cells. (D) Quantification of cell migration number in U87 and U251 cells. (E) Cell invasion ability was detected by Transwell chamber assay. All data were presented as mean ± SD from three biological replicates. *$p < 0.01$ using one-way ANOVA followed by Tukey post hoc test.

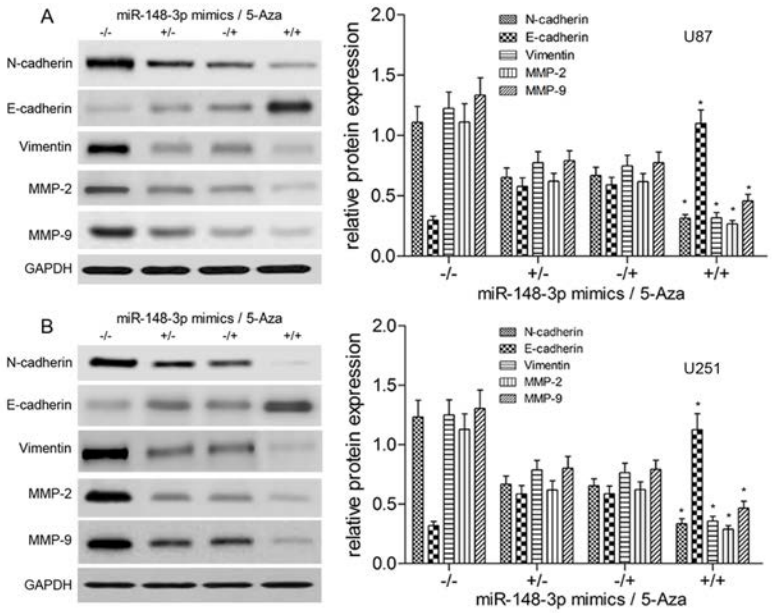

Figure 6. Mediation of epithelial–mesenchymal transition (EMT) pathway activity by miR-148-3p or 5-Aza. (A) Western blot bands of N-cadherin, E-cadherin, vimentin, MMP-2, and MMP-9 in U87 cells and semiquantification of relative protein expression after miR-148-3p mimics transfection and/or 5-Aza treatment in U87 cells. (B) Western blot bands of N-cadherin, E-cadherin, vimentin, MMP-2, and MMP-9 in U251 cells, and semiquantification of relative protein expression after miR-148-3p mimics transfection and/or 5-Aza treatment in U251 cells. All data were presented as mean ± SD from three biological replicates. $*p < 0.01$ using one-way ANOVA followed by Tukey post hoc test.

types of cancers, and miR-148-3p is believed to act as a tumor suppressor. However, the expression and role of miR-148-3p in GBM need to be further studied. In the present study, we found that miR-148-3p can modulate the DNMT1–RUNX3 axis and EMT pathway, which can mediate invasion, migration, and apoptosis of GBM cells (Fig. 7).

In our study, the expression of miR-148-3p in glioma tissues was decreased and correlated with WHO grade, tumor size, and prognosis as well as DNMT1 and RUNX3 expressions. Furthermore, miR-148-3p expression in GBM cells was also downregulated, accompanied with DNMT1 upregulation and RUNX3 downregulation compared with NHA cells. The results indicated that the miR-148-3p–DNMT1–RUNX3 axis may be involved in the development of GBM. Previous studies demonstrated that the regulation of the tumor suppressor gene is frequently modulated by some types of miRNAs. For example, increased expression of miR-21 and miR-146b is related to loss of DNA methylation in papillary thyroid carcinoma[22]. miR-503 cluster is coordinately underexpressed in endometrial endometrioid adenocarcinoma and targets many oncogenes, cell cycle genes, DNA repair genes, and chemotherapy-response genes[23]. On the other hand, miRNA expression is also subjected to the epigenetic regulatory network during tumor progression[24], which can be downregulated by DNA methylation. Thus, the interaction between miRNAs and DNA methylation may play a crucial role in the progression of GBM.

Based on the findings above, the relationship among miR-148-3p, DNMT1, and RUNX3 in cell lines was further determined. First, 5-Aza as a putative strong DNA demethylation reagent was applied as a positive control[25]. We found that 5-Aza suppressed DNMT1 expression and repressed methylation of RUNX3 gene promoter region, leading to upregulated RUNX3 expression. In addition, 5-Aza inhibited the migration and invasion of GBM cells. Then we conducted transfection with miR-148-3p mimics and demonstrated that miR-148-3p mimics also downregulated DNMT1 and suppressed methylation of

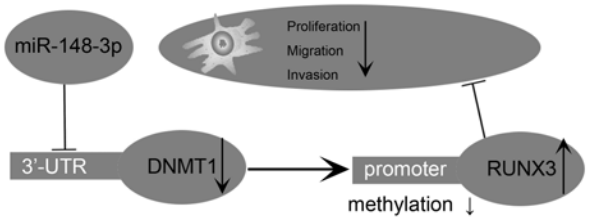

Figure 7. The schematic summaries of the relationship of miR-148-3p, DNMT1, RUNX3, and GBM cell proliferation/migration/invasion.

RUNX3 promoter region, which upregulated RUNX3 expression. As known to all, RUNX3 suppressed tumor cell migration and invasion, or enhanced cell apoptosis[26,27]. Our study also identified that demethylation of RUNX3 promoted its expression and exerted its tumor suppressor effects. To further explore potential molecular mechanisms of miR-148-3p in mediating cell migration and invasion, we detected the expressions of EMT biomarkers, and found that miR-148-3p mimics upregulated epithelial-related protein and downregulated mesenchymal proteins, thus impeding EMT processes.

In conclusion, our results indicated miR-148-3p as a tumor suppressor of GBM. miR-148-3p targeted 3 - UTR of DNMT1 to inhibit the expression of DNMT1, and decreased methylation of the tumor suppressor gene RUNX3, by which miR-148-3p suppressed cell migration or invasion, and induced apoptosis and cell cycle arrest. The present study indicates the potential value of miR-148-3p as a potential biomarker of GBM or a pharmaceutical target in the future.

ACKNOWLEDGMENT: The authors declare no conflicts of interest.

REFERENCES

1. Desjardins A, Gromeier M, Herndon JE 2nd, Beaubier N, Bolognesi DP, Friedman AH, Friedman HS, McSherry F, Muscat AM, Nair S, Peters KB, Randazzo D, Sampson JH, Vlahovic G, Harrison WT, McLendon RE, Ashley D, Bigner DD. Recurrent glioblastoma treated with recombinant poliovirus. N Engl J Med. 2018;379:150–61.
2. Kim SH, Yoo H, Chang JH, Kim CY, Chung DS, Kim SH, Park SH, Lee YS, Yang SH. Procarbazine and CCNU chemotherapy for recurrent glioblastoma with MGMT promoter methylation. J Korean Med Sci. 2018;33:e167.
3. Rennert RC, Khan U, Tatter SB, Field M, Toyota B, Fecci PE, Judy K, Mohammadi AM, Landazuri P, Sloan A, Leuthardt E, Chen CC. Patterns of clinical use of stereotactic laser ablation: Analysis of a multicenter prospective registry. World Neurosurg. 2018;116:e566–70.
4. Kirkin AF, Dzhandzhugazyan KN, Guldberg P, Fang JJ, Andersen RS, Dahl C, Mortensen J, Lundby T, Wagner A, Law I, Broholm H, Madsen L, Lundell-Ek C, Gjerstorff MF, Ditzel HJ, Jensen MR, Fischer W. Adoptive cancer immunotherapy using DNA-demethylated T helper cells as antigen-presenting cells. Nat Commun. 2018;9:785.
5. Jackson S, Weingart J, Nduom EK, Harfi TT, George RT, McAreavey D, Ye X, Anders NM, Peer C, Figg WD, Gilbert M, Rudek MA, Grossman SA. The effect of an adenosine A2A agonist on intra-tumoral concentrations of temozolomide in patients with recurrent glioblastoma. Fluids Barriers CNS 2018;15:2.
6. Straube C, Scherb H, Gempt J, Kirschke J, Zimmer C, Schmidt-Graf F, Meyer B, Combs SE. Adjuvant stereotactic fractionated radiotherapy to the resection cavity in recurrent glioblastoma—the GlioCave study (NOA 17 - ARO 2016/3 - DKTK ROG trial). BMC Cancer 2018;18(1):15.
7. Yang N, Zhu S, Lv X, Qiao Y, Liu YJ, Chen J. MicroRNAs: Pleiotropic regulators in the tumor microenvironment. Front Immunol. 2018;9:2491.
8. Huang S, Tan X, Huang Z, Chen Z, Lin P, Fu SW. MicroRNA biomarkers in colorectal cancer liver metastasis. J Cancer 2018;9:3867–73.
9. Cao H, Liu Z, Wang R, Zhang X, Yi W, Nie G, Yu Y, Wang G, Zhu M. miR-148a suppresses human renal cell carcinoma malignancy by targeting AKT2. Oncol Rep. 2017;37:147–54.
10. Luo Q, Li W, Zhao T, Tian X, Liu Y, Zhang X. Role of miR-148a in cutaneous squamous cell carcinoma by repression of MAPK pathway. Arch Biochem Biophys. 2015;583:47–54.
11. Jili S, Eryong L, Lijuan L, Chao Z. RUNX3 inhibits laryngeal squamous cell carcinoma malignancy under the regulation of miR-148a-3p/DNMT1 axis. Cell Biochem Funct. 2016;34:597–605.
12. Zhou D, Wan Y, Xie D, Wang Y, Wei J, Yan Q, Lu P, Mo L, Xie J, Yang S, Qi X. DNMT1 mediates chemosensitivity by reducing methylation of miRNA-20a promoter in glioma cells. Exp Mol Med. 2015;47:e182.
13. Sun J, Tian X, Zhang J, Huang Y, Lin X, Chen L, Zhang S. Regulation of human glioma cell apoptosis and invasion by miR-152-3p through targeting DNMT1 and regulating NF2: MiR-152-3p regulate glioma cell apoptosis and invasion. J Exp Clin Cancer Res. 2017;36:100.
14. Seelan RS, Mukhopadhyay P, Pisano MM, Greene RM. Effects of 5-Aza-2'-deoxycytidine (decitabine) on gene expression. Drug Metab Rev. 2018;50:193–207.
15. Marco MD, Ramassone A, Pagotto S, Anastasiadou E, Veronese A, Visone R. MicroRNAs in autoimmunity and hematological malignancies. Int J Mol Sci. 2018;19:E3139.
16. Xie M, Ma L, Xu T, Pan Y, Wang Q, Wei Y, Shu Y. Potential regulatory roles of microRNAs and long noncoding RNAs in anticancer therapies. Mol Ther Nucleic Acids 2018;13:233–43.
17. Xu X, Tao Y, Shan L, Chen R, Jiang H, Qian Z, Cai F, Ma L, Yu Y. The role of microRNAs in hepatocellular carcinoma. J Cancer 2018;9:3557–69.
18. Sun Z, Shi K, Yang S, Liu J, Zhou Q, Wang G, Song J, Li Z, Zhang Z, Yuan W. Effect of exosomal miRNA on cancer biology and clinical applications. Mol Cancer 2018; 17:147.
19. Hibner G, Kimsa-Furdzik M, Francuz T. Relevance of microRNAs as potential diagnostic and prognostic markers in colorectal cancer. Int J Mol Sci. 2018;19:E2944.
20. Yu H, Guan Z, Cuk K, Brenner H, Zhang Y. Circulating microRNA biomarkers for lung cancer detection in Western populations. Cancer Med. 2018;7:4849–62.
21. Wang RH, He LY, Zhou SH. The role of gene sculptor microRNAs in human precancerous lesions. Onco Targets Ther. 2018;11:5667–75.
22. Ortiz IMDP, Barros-Filho MC, Dos Reis MB, Beltrami CM, Marchi FA, Kuasne H, do Canto LM, de Mello JBH, Abildgaard C, Pinto CAL, Kowalski LP, Rogatto SR. Loss of DNA methylation is related to increased expression of miR-21 and miR-146b in papillary thyroid carcinoma. Clin Epigenetics 2018;10:144.
23. Devor EJ, Cha E, Warrier A, Miller MD, Gonzalez-Bosquet J, Leslie KK. The miR-503 cluster is coordinately underexpressed in endometrial endometrioid adenocarcinoma and targets many oncogenes, cell cycle genes, DNA repair genes and chemotherapy response genes. Onco Targets Ther. 2018; 11:7205–11.
24. Zhang W, Chen JH, Shan T, Aguilera-Barrantes I, Wang LS, Huang TH, Rader JS, Sheng X, Huang YW. miR-137 is a

tumor suppressor in endometrial cancer and is repressed by DNA hypermethylation. Lab Invest. 2018;98:1397–407.
25. Numoto K, Yoshida A, Sugihara S, Kunisada T, Morimoto Y, Yoneda Y, Fujita Y, Nishida K, Ouchida M, Ozaki T. Frequent methylation of RASSF1A in synovial sarcoma and the anti-tumor effects of 5-aza-2'-deoxycytidine against synovial sarcoma cell lines. J Cancer Res Clin Oncol. 2010; 136:17–25.
26. Sun J, Li B, Jia Z, Zhang A, Wang G, Chen Z, Shang Z, Zhang C, Cui J, Yang W. RUNX3 inhibits glioma survival and invasion via suppression of the -catenin/TCF-4 signaling pathway. J Neurooncol. 2018;140:15–26.
27. Bai X, Han G, Liu Y, Jiang H, He Q. MiRNA-20a-5p promotes the growth of triple-negative breast cancer cells through targeting RUNX3. Biomed Pharmacother. 2018; 103:1482–9.